

JPET #178079

The Journal of Pharmacology and Experimental Therapeutics

Title page

Involvement of matrix metalloproteinase-mediated proteolysis of neural cell adhesion molecule in the development of cerebral ischemic neuronal damage

Kanako Shichi, Wakako Fujita-Hamabe, Shinichi Harada, Hiroyuki Mizoguchi, Kiyofumi Yamada, Toshitaka Nabeshima and Shogo Tokuyama

Department of Clinical Pharmacy, Kobe Gakuin University School of Pharmaceutical Sciences (K.S., W.F.H., S.H., S.T.)

Futuristic Environmental Simulation Center, Research Institute of Environmental Medicine, Nagoya University (H.M.)

Department of Neuropsychopharmacology and Hospital Pharmacy, Nagoya University Graduate School of Medicine (K.Y.)

Comparative Cognitive Science Institutes and Department of Chemical Pharmacology, Meijo University, Graduate School of Pharmaceutical Science (T.N.)

JPET #178079

Running title page

Running title: Neural cell adhesion molecule and neuronal death

Corresponding author: Shogo Tokuyama

Department of Clinical Pharmacy, Kobe Gakuin University School of Pharmaceutical

Sciences, 1-1-3 Minatojima, Chuo-ku, Kobe 650-8586, Japan

Tel and Fax: +81-78-974-4780

E-mail: stoku@pharm.kobegakuin.ac.jp

Number of text pages: 43

Number of tables: 0

Number of figures: 7

Number of references: 47

Number of words in the Abstract: 201

Number of words in the Introduction: 471

Number of words in the Discussion: 1356

JPET #178079

Abbreviations: MMP, matrix metalloproteinase; NCAM, neural cell adhesion molecule;
MCAO, middle cerebral artery occlusion; CCA, common carotid artery; ECA, external
carotid artery; ICA, internal carotid artery; rCBF, relative cerebral blood flow; TTC,
2,3,5-triphenyltetrazolium chloride; NDS, neurological deficit score.

Section: Cellular and Molecular

Abstract

Neural cell adhesion molecule (NCAM) is a membrane protein abundantly expressed in the central nervous system. Recently, it has been reported that dysfunction of NCAM is linked to human brain disorders. Furthermore, NCAM is one of the proteolysis targets of matrix metalloproteinase (MMP), whose activation is implicated in neuronal damage. The aim of this study was to elucidate an involvement of MMP-mediated proteolysis of NCAM in the development of ischemic neuronal damage. Male ddY and MMP-9 knock-out (KO) C57BL/6J mice were subjected to 2 h of middle cerebral artery occlusion (MCAO). In MCAO model mice, development of infarction and behavioral abnormality were clearly observed on day 1 and day 3 after MCAO. Protein levels of MMP-2 and MMP-9 were significantly increased on day 1 and day 3 after MCAO. In addition, full-length of NCAM (180 kDa) was significantly decreased, but its metabolite levels increased on day 1 by ischemic stress per se. NCAM siRNA significantly increased the neuronal damage induced by MCAO. MMP inhibition or MMP-9 gene knockout attenuated the infarction, behavioral abnormalities and decrease of NCAM (180kDa) observed after MCAO in mice. The present findings clearly suggest that MMP-2/MMP-9-mediated NCAM proteolysis is implicated in the exacerbation of ischemic neuronal damage.

Introduction

Focal cerebral ischemia (stroke) is the third most common cause of death in the world (Hankey and Warlow, 1999; Hasegawa et al., 2006). The ischemic neuronal damage is known to be related to mitochondria and endoplasmic reticulum dysfunction, activated oxygen species, increased expression of inflammatory cytokines and proteolytic enzymes (Heo et al., 1999; Zhao et al., 2004; Sarabi et al., 2008), while the detailed molecular mechanisms are still unknown. In spite of the development of various therapeutic strategies including thrombolysis with tissue-type plasminogen activator (tPA) or free radical scavengers (Yepes et al., 2000), it has been difficult to completely cure because of the intractable severe subsequent complications such as paralysis and cognitive dysfunction (Shinohara et al., 2009; Yagi et al., 2009). Thus, clarification of the detailed mechanisms responsible for the development of ischemic neuronal damage is urgently required. The aim of this study was to identify one of the key molecules involved in the ischemic neuronal damage.

Neuronal cell adhesion molecule (NCAM), a member of the immunoglobulin superfamily of cell recognition molecules, is expressed on the membranes of neurons and glial cells and promotes cell-cell interaction via homophilic and heterophilic binding (Povlsen et al., 2003; Maness and Schachner, 2007). Importantly, NCAM is known to

regulate these processes which influence cell adhesion, cell migration, and neurite outgrowth and be involved in development of the nervous system, in brain plasticity associated with learning and memory, and in neuronal regeneration (Maness and Schachner, 2007). Furthermore, dysfunction of NCAM is reported to contribute to the development of neurological disorders such as schizophrenia, bipolar disorder and Alzheimer's disease (Vawter, 2000; Todaro et al., 2004; Maness and Schachner, 2007).

NCAM is synthesized in three main membrane-bound isoforms, NCAM-120, NCAM-140, and NCAM-180 (Ronn et al., 1998). Interestingly, among these isoforms, the proteolysis of NCAM-180 has been reported to relate to psychological disorders in humans (Poltorak et al., 1996; Vawter, 2000; Tanaka et al., 2007). In addition, mice lacking NCAM-180 have deficits in learning, emotional memory, and sensory gating (Bukalo et al., 2004; Maness and Schachner, 2007). Recently, matrix metalloproteinase (MMP), one of the proteolytic enzymes targeting NCAM (Hubschmann et al., 2005; Hinkle et al., 2006), is reported to be activated by ischemic stress (Heo et al., 1999; Zhao et al., 2004). Although some target molecules of MMP such as laminin or IL-1 β are reported to be involved in neuronal death and/or development of neuronal injury (Gu et al., 2005; Kawasaki et al., 2008), there are no reports indicating that the MMP-NCAM interaction is involved in the development of neuronal damage. Here, we focused on the

JPET #178079

involvement of MMP-mediated proteolysis of NCAM in the development of ischemic neuronal damage using middle cerebral artery occlusion (MCAO) model mice, a popular ischemic model in experimental stroke research that results in prominent ischemic damage as we described previously (Harada et al., 2009).

JPET #178079

Methods

Animals

The experiments were performed on male ddY mice (5–6 weeks old, SLC, Osaka, Japan) and MMP-9 KO (background of C57BL/6J) mice were kindly given by Nagoya University Research Institute of Environmental Medicine (Nagoya, Japan). As previously described (Mizoguchi et al., 2007), MMP-9 homozygous KO mice (10-12-weeks old) were obtained from the Jackson Laboratory (Bar Harbor, ME, USA), and crossed to C57BL/6J mice for eight generations before being made homozygous. Wild type C57BL/6J mice were obtained from the Japan SLC (Osaka, Japan). The animals were housed at a temperature of 23–24°C with a 12-h light–dark cycle (lights on 8:00 a.m. to 8:00 p.m.). Food and water were available ad libitum. The present study was conducted in accordance with the Guiding Principles for the Care and Use of Laboratory Animals, adopted by the Japanese Pharmacological Society. In addition, all experiments were approved by the ethical committee for animals of Kobe Gakuin University (approval number: A 060601-10).

Drug treatments

GM6001

JPET #178079

{N-[(2R)-2(Hydroxamidocarbonylmethyl)-4-methylpentanoyl]-L-tryptophan Methylamide}, a broad-spectrum MMP inhibitor (Calbiochem, CA, USA), and selective MMP-2 and MMP-9 inhibitors, MMP-2 inhibitor III [(2-((Isopropoxy)-(1, 1'-biphenyl-4-ylsulfonyl)-amino))-N-hydroxyacetamide] (Calbiochem) and MMP-9 inhibitor I [4-methoxyphenyl benzyl(4-((diethylamino)methyl)-2-(hydroxycarbamoyl)-6-methylphenyl)sulfite] (Calbiochem), respectively, were dissolved in 4% DMSO in saline (0.5 µg/µL) and administered in a volume of 5 µg/mouse through the intracerebroventricular (i.c.v.) route 30 min before and 2 h after ischemia. Control mice were administered 4% DMSO in saline (vehicle) in a volume of 10 µl/mouse (i.c.v.). NCAM1 ON-TARGET^{plus} SMART pool (NCAM siRNA; Thermo Fisher Scientific, Kanagawa, Japan), ON-TARGET^{plus} Non-targeting Pool (Control siRNA; Thermo Fisher Scientific), and *in vivo* jetPEI™ + 10% Glucose (Cationic polymer transfection reagent; Polyplus-transfection, NY, USA) were administered directly after preparation. Mice were injected with siRNA directed at NCAM (1 µg/mouse, i.c.v.) 72 h before MCAO to knock down NCAM protein levels. I.c.v. administrations were performed as previously described (Haley and McCormick, 1957). Briefly, a microsyringe with a 27-gauge stainless-steel needle was used for all experiments. Tubing covered all but the terminal 2.5 to 3.0 mm of the needle so as to

JPET #178079

make a track through the brain and into the lateral ventricle but not through the floor of the lateral ventricle. The needle inserted unilaterally into the lateral ventricle of the brain (1.0 mm lateral and 1.0 mm posterior to the bregma) as previously described (Franklin and Paxions, 2008). Verification of needle position in the lateral cerebroventricle was made by i.c.v. dye injection and subsequent post-mortem brain section verification of dye placement.

Induction of ischemic/reperfusion injury

The experimental transient focal ischemia mouse model was generated by performing MCAO as described previously (Harada et al., 2009). Briefly, mice were anesthetized with 2% isoflurane (Abbott Japan, Osaka, Japan) and maintained in an anesthetized state with 1% isoflurane. The rectal temperature was maintained at $37 \pm 0.5^{\circ}\text{C}$ with the use of a heating blanket (FH-100, Unique Medical, Osaka, Japan) that was feedback controlled by a rectal temperature probe (PTE-101, Unique Medical) and a small animal heat controller (ATC-101B, Unique Medical). The left common carotid artery (CCA) and external carotid artery (ECA) underwent a midline pretracheal incision. The vagus nerves were separated carefully from the artery. CCA and ECA were ligated, and then the internal carotid artery (ICA) was isolated. Bifurcation of the CCA was made

JPET #178079

through a small incision, and then a 8-0 nylon monofilament (Shirakawa, Fukushima, Japan) with a 4-mm tip coated in silicon resin (Xantopren Blue and Activator, Heraeus Kulzer, Hanau, Germany) was introduced through a small incision and was advanced 9 mm along the ICA beyond the bifurcation site, thus stopping the blood flow to the middle cerebral artery (MCA). After 2 h of ischemia, mice were re-anesthetized with isoflurane; then, the filament was withdrawn for blood reperfusion. The sham-operated mice were subjected to the procedure mentioned above without MCAO. The operative site was sutured and mice were allowed to awake from the anesthesia. Mice with brain hemorrhage were eliminated from analysis. The relative cerebral blood flow (rCBF) was measured by laser Doppler flowmetry (LDF; TBF-LN1, Unique Medical) to assess the adequacy of the vascular occlusion and reperfusion, as described previously (Harada et al., 2009).

Measurement of infarct volume

Mice were euthanized by cervical dislocation on day 1 and day 3 after MCAO. The brains were cut into 2-mm thick coronal slices (-2, 0, +2 and +4 mm from the bregma) using a brain slicer. The brain slices were then incubated in normal saline containing 2% 2,3,5-triphenyltetrazolium chloride (TTC; Sigma, MO, USA) for 10 min

JPET #178079

at 37°C. After staining, the brain slices were fixed with 4% paraformaldehyde (Sigma) for 2 h, and then stored in phosphate-buffered saline. Areas not stained red with TTC were considered to be infarctions. The brain slices were scanned. Unstained areas (infarct areas) were measured using image analysis software (Image J (NIH, MD, USA) and Adobe Photoshop Elements 5.0 (Adobe Systems Incorporated, Tokyo, Japan). The infarct volume (mm³) was calculated by multiplication of infarct volume (mm³) and intensity (intensity = intensity of left hemisphere – intensity of right hemisphere).

Measurement of brain edema

Brain edema was assessed by measuring the brain water content according to the wet-dry method as described previously (Ding-Zhou et al., 2003; Liu et al., 2008). Briefly, after decapitation, the brain was quickly removed and dissected along the interhemispheric fissure into the ischemic and nonischemic cerebral hemispheres. Tissues were weighed with a scale to within 0.1 mg. Dry weight of the brain was determined after heating the tissue for 3 days at 100°C in a drying oven. Brain water content was then calculated as [(wet weight - dry weight)/wet weight] x 100.

Neurological examination

Neurological examination was performed using the neurological deficit score (NDS) comprising consciousness (0, normal; 1, restless; 2, lethargic; 3, stuporous; 4, seizures; and 5, death), walking (0, normal; 1, paw; 2, unbalanced walking; 3, circling; 4, unable to stand; and 5, no movement), and limb tone (0, normal; 1, spastic; and 2, flaccid), and pain reflex was scored after reperfusion as described previously (Harada et al. 2009). Pain reflex was assessed using the tail flick test (pain reflex = latency after MCAO – latency before MCAO). A cut-off time of 10 s was used to prevent any injury to the tail.

Western blot analysis

On indicated days after reperfusion, mice were decapitated and brains were removed. Ipsilateral cortex was dissected, and homogenized with homogenize buffer (20 mM Tris-HCl, pH 7.5, 120 mM NaCl, 4% Tween-20, 2 mM β -mercaptoethanol, 1 mM Na_3VO_4 , 5 mM benzamidine, 20 mM NaF, 1 mM *p*-nitrophenyl phosphate, 5 mM imidazole, 50 mg/ml trypsin inhibitor, 50 mg/ml leupeptin, 50 mg/ml aprotinin, 5 mg/ml pepstatin, 1 mM PMSF). After centrifugation at 15000 *g*, the supernatant was collected and immediately lysed in SDS-sample buffer (50 mM Tris-HCl, pH 6.8, 2% SDS, 10% glycerol), boiled and reduced with β -mercaptoethanol. To investigate protein expression

JPET #178079

patterns in control and ischemic cortex, equal amounts (20 µg) of total protein extracts were prepared. After mixing with 2× sample buffer, each sample was separated by non-reducing gel in native condition for NCAM, MMP-2 and MMP-9 (120 V, 90 min). Markers used were Precision Plus Protein Standards Kaleidoscope (Bio-Rad, CA, USA). After separation, proteins were transferred to nitrocellulose membranes (15 V, 50 min). All blots were blocked with 10% skim milk (blocking agent; GE Healthcare, Osaka, Japan) in PBS, pH 7.4, or in TBS, containing 0.1% Tween 20 (PBS-T or TBS-T) at room temperature for 1 h. Then, the membranes were incubated with the primary antibodies diluted in blocking buffer at 4°C overnight. The dilution rates of the primary antibodies were 1:200, 1:1000, 1:1000, and 1:20,000 for NCAM (65 and 180 kDa) (Sigma), MMP-2 (Abcam, Tokyo, Japan), MMP-9 (Cell Signaling, Tokyo, Japan), and GAPDH (Millipore, Temecula, CA, USA), respectively. After washing with PBS-T or TBS-T for 30 min, the membrane was incubated with secondary antibody [HRP-labeled affinity purified antibody to rabbit IgG+IgM (H+L) (1:1000; Fitzgerald, NA, U.S.A.) for MMP-2 and MMP-9, HRP-labeled affinity purified antibody to mouse IgG+IgM (H+L) (1:10,000; Thermo Fisher Scientific, Tokyo, Japan) for NCAM (65 and 180 kDa) and GAPDH] at room temperature for 40 min. After washing with PBS-T or TBS-T for 30 min, antigen was detected by using the standard chemical luminescence method (ECL™, GE

JPET #178079

Healthcare). Detection of band was used by Light-Capture II (ATTO, Tokyo, Japan) and Cs-Analyzer (ver. 3.0, ATTO).

Gelatin Zymography

Similarly prepared protein samples (as in Western blot analysis) were incubated with 50% gelatin sepharose 4B (GE Healthcare, Osaka, Japan) for 4 h. After washing with wash buffer (50 mM Tris-HCl (pH 7.6), 150 mM NaCl, 5 mM CaCl₂, 0.05% BRIJ-35, 0.02% NaN₃), samples were eluted by elution buffer (50 mM Tris-HCl (pH 7.6), 150 mM NaCl, 5 mM CaCl₂, 0.05% BRIJ-35, 0.02% NaN₃, 10% DMSO). After centrifugation for 30 min at 4°C, supernatant was loaded and separated in a precast gel by use of Gelatin-zymography kit (Primary Cell, Hokkaido, Japan). After separation by electrophoresis, the gel was renatured and then incubated with developing buffer at 37°C over 60 h. After developing, the gel was stained with 0.5% Coomassie Blue R-250 for 30 min and then destained appropriately in methanol and acetic acid in water (30:5:65). Detection of band was used by Light-Capture II (ATTO, Tokyo, Japan) and Light Viewer SLIM 57 (ATTO). Semi-quantified analysis of band intensity was performed using Image J (National Institutes of Health, Bethesda, MD, U.S.A.).

Statistical analysis

Data are presented as means \pm S.E.M. Comparisons of parameters at a given time point among multiple treatment groups, as well as within treatment group comparisons across more than two time points were conducted using a one-way analysis of variance, followed by a post hoc Dunnett test or Scheffe's test. Comparisons of parameters measured in absence versus presence of treatment were conducted using unpaired Student's *t* test. The data for NDS were analyzed using a Steel-Dwass test of post-hoc nonparametric multiple comparison tests or by a Wilcoxon-Mann-Whitney U test. Data are presented as medians (25th -75th percentile). Before statistical post hoc test, we have checked normality and equal variance test for all data. The differences were regarded as statistically significant when the *p* value was less than 0.05.

Results

Development of neuronal damage and protein levels or activity of MMP-2 and MMP-9 in the cerebral cortex after cerebral ischemic stress

As shown in Fig. 1A, the infarct area in the cortex, hippocampus and striatum was gradually enlarged on day 3 compared with on day 1 after MCAO (Fig. 1A, B). In addition, the increase of brain water content, indicating the development of edema, was significantly observed and gradually enlarged on day 1 and day 3 after MCAO (Fig. 1C). In addition, NDS was significantly increased in the MCAO group than in the sham group on day 1 and day 3 (Fig. 1D). In the western blot analysis, we detected a 72 kDa band for MMP-2 and 108 kDa band for MMP-9, and they were significantly increased on day 1 and day 3 after MCAO compared with the sham group (Fig. 1E, F). The gelatin zymograms clearly demonstrated the increase of MMP-2 and MMP-9 activity on day 3 after MCAO. Semi-quantified data showed the significant differences, in a GM6001, a broad range MMP inhibitor, -reversible manner (Fig. 1G).

Effect of NCAM siRNA on ischemic neuronal damage

To confirm the role of NCAM in MCAO-induced neuronal damage, we investigated whether NCAM knockdown increases the ischemic neuronal damage. Three

JPET #178079

days after NCAM siRNA administration, NCAM (180 kDa) protein levels were significantly decreased in the cortex in naïve mice (Fig. 2A). In addition, we confirmed the NCAM (180 kDa) protein levels were kept lower until 4 days after siRNA administration (data not shown). Thus, we performed MCAO on day 3 after NCAM siRNA administration.

The infarct volume was significantly increased on day 1 after MCAO in the NCAM siRNA-treated group compared with the control group (Fig. 2B, C). NDS was also significantly increased in the NCAM siRNA-treated group than in the control group (Fig. 2D). Since the development of infarction accomplishes maximum on day 3 after MCAO, it was hard to compare the difference between control and siRNA-treated group on day 3 after MCAO.

Protein levels of NCAM (180 kDa) and NCAM cleavage product (65 kDa) after cerebral ischemic stress

Since NCAM is one of the proteolysis targets of matrix metalloproteinase (MMP), the levels of NCAM (180 kDa) and NCAM cleavage product (65 kDa) after cerebral ischemic stress were determined. NCAM (180 kDa) protein levels were significantly decreased on day 1 after MCAO compared with the sham group, while it

JPET #178079

returned to the sham levels on day 3 (Fig. 3A). On the other hand, NCAM cleavage product levels (65 kDa) were significantly increased on day 1 and day 3 compared with the sham group (Fig. 3B).

Effect of a non-selective MMP inhibitor, GM6001, on ischemic neuronal damage, NCAM protein levels and NCAM cleavage product levels

We investigated whether MMP inhibitor suppresses the development of ischemic neuronal damage. As shown in Fig. 4A and B, the infarct volume observed on day 3 after MCAO was significantly decreased by treatment of GM6001 (Fig. 4). Furthermore, the ischemic stress-induced an increase of NDS was also significantly inhibited by GM6001 treatment (Fig. 4C). In addition, the decrease in NCAM (180 kDa) protein levels observed on day 1 were completely recovered to the control level by GM6001 (Fig. 4D). In addition, the increment of NCAM cleavage product levels (65 kDa) observed on day 1 and day 3 was significantly suppressed by GM6001 (Fig. 4E).

Effect of MMP isozyme-specific inhibitors on ischemic neuronal damage, NCAM protein levels and NCAM cleavage product levels

To determine which MMP plays critical role in MCAO, we used selective

JPET #178079

inhibitors for MMP-2 and MMP-9. The development of infarction and increase of NDS observed on day 3 was significantly decreased by the MMP-2 inhibitor III (Fig. 5A, B, and C). The decrease in NCAM (180 kDa) protein levels observed on day 1 was completely recovered to the control level by MMP-2 inhibitor III (Fig. 5D). In addition, the increment of NCAM cleavage product levels (65 kDa) observed on day 1 and day 3 were significantly suppressed by this inhibitor (Fig. 5E). Furthermore, treatment with the selective MMP-9 inhibitor I, showed the same results as the selective MMP-2 inhibitor III (Fig. 6).

Ischemic neuronal damage and NCAM protein levels, NCAM cleavage product levels after cerebral ischemic stress in MMP-9 KO mice

To confirm the role of MMP-9 in MCAO, we investigated whether MCAO shows ischemic neuronal damage using MMP-9 KO mice. Since C57BL/6 strain is known to be more susceptible to cerebral ischemia when compared to ddY mice (Yang et al., 1997), here, we investigated only on day 1 after MCAO. The development of infarction was significantly reduced in the MMP-9 KO mice compared with WT mice on day 1 after MCAO (Fig. 7A and B). The NDS on day 1 was also significantly decreased in the MMP-9 KO mice compared with WT mice (Fig. 7C). In addition, the decrease in

JPET #178079

NCAM (180 kDa) protein levels and increment of NCAM cleavage product levels (65 kDa) in WT mice were not observed in the MMP-9 KO mice on day 1 after MCAO (Fig. 7D, E).

Discussion

NCAM, one of the members of the immunoglobulin superfamily of CAMs, is encoded by a single gene located in chromosome 11 in humans. As a result of alternative splicing, three types of isoforms are known as NCAM-180 (180 kDa), NCAM-140 (140 kDa), and NCAM-120 (120 kDa), which differ in their C-terminals (intracellular part) (Tacke and Goridis, 1991; Doherty et al., 2000). NCAM is widely expressed in the nervous system where it plays a pivotal role in proliferation, migration, axonal outgrowth, fasciculation and synaptic plasticity (Ronn et al., 1998; Berezin et al., 2000; Povlsen et al., 2003; Maness and Schachner, 2007). Furthermore, NCAM is found on glial and neuronal cells and participates in binding these cells together (Vawter, 2000). It has been suggested that neuron-glia interactions are involved in the physiological function of neurons (Vawter, 2000; Chadi et al., 2009). Aside from its role in cell-cell interactions, an important role for NCAM in regulation of intracellular signaling pathways has been revealed (Povlsen et al., 2003; Kiryushko et al., 2004).

Recently, the protein levels of NCAM and its post-translational modified form polysialylated NCAM, have been reported to be highly susceptible to modulation by stress (Bisaz et al., 2009). In regard to cerebral ischemic stress, the increase of polysialylated-NCAM was observed in the subventricular zone that is involved in the

JPET #178079

proliferation of endogenous neural progenitor cells (Macas et al., 2006), while there are no reports about the alteration of NCAM per se. We focused on NCAM-180, the largest isoform of NCAM that possesses the full size of cytoplasmic termini. Interestingly, we found that ischemic stress per se induced down-regulation of full length of NCAM (180 kDa) in the cortex. It is possible that down-regulation of full length of NCAM (180 kDa) becomes one of the triggers of neuronal damage under ischemic stress.

In this study, we clearly confirmed that down-regulation of NCAM by siRNA significantly exacerbated the neuronal damage in MCAO model mice. These findings suggest that NCAM possesses a surviving effect on the CNS. Previous reports have demonstrated that NCAM deficiency causes morphological alterations in the CNS, including a reduction in brain weight and the size of the olfactory bulb (Cremer et al., 1994). These results may correlate with our observations that show the importance of NCAM in neuronal survival. Furthermore, many reports have indicated that NCAM KO mice leads to impaired long-term potentiation (Cremer et al., 1998), severe cognitive impairments and emotional alterations (Cremer et al., 1994; Bisaz et al., 2009), suggesting the importance of NCAM in brain function. As we have previously reported, the post-ischemic memory dysfunction could be developed in this MCAO model (Harada et al., 2009; Harada et al., 2010). It is possible that down-regulation of full-length of

NCAM (180 kDa) may be involved in the post-ischemic memory dysfunction.

The ischemic stress induced not only the decrease of full length of NCAM (180 kDa), but also the increase of NCAM cleavage product (65 kDa), which is considered a proteolytic fragment of NCAM (Tanaka et al., 2007) by extracellular proteases. MMP is a family of zinc-dependent endopeptidases that can be released or activated in a neuronal activity dependent manner (Mizoguchi et al., 2007) and are attractive targets in the field of inflammatory and psychological diseases (Yong et al., 2001; Kawasaki et al., 2008; Mizoguchi et al., 2008). They cleave all constituents of the ECM including collagens and laminins (Yong et al., 2001). Recently, it has been well known that MMPs can also target a variety of non matrix proteins including varied soluble molecules, cell surface receptors and synaptic cell adhesion molecules (CAMs) including NCAM (Vawter, 2000; Conant et al., 2010). The soluble extracellular domain of NCAM has been identified in normal brain, potentially arising from ectodomain shedding of the extracellular domain of transmembrane NCAM by MMPs (Hubschmann et al., 2005; Hinkle et al., 2006).

There are at least 25 members of the MMP family and their activity is tightly regulated. Although MMPs are expressed in both glial and neuronal cell (Yong et al., 2001; Szklarczyk et al., 2002), ischemic stress is known to induce MMP-2 and MMP-9, major isozymes in the MMP family, in glial cells such as reactive microglia and

astrocytes (Svedin et al., 2007). Ischemic stress accompanies the progression of neuronal death via cleavage of precursors of inflammatory cytokines by MMP-2 and MMP-9 (Amantea et al., 2007; del Zoppo et al., 2007).

In this study, MMP-2 and MMP-9 were significantly up-regulated on day 1 and day 3 after ischemic stress. The increased enzymatic activity of MMP-2 and MMP-9 was also detected on day 3 after ischemic stress, corresponding with the previous studies (Asahi et al., 2001; Lee et al., 2004; Koistinaho et al., 2005). Since the increase of full length NCAM (180 kDa) was accompanied by the decrease of NCAM cleavage product (65 kDa) by an inhibition of MMP-2 and MMP-9, these changes seem to be due to the transmembrane proteolysis of NCAM via activation of these enzymes. Furthermore, the present results using MMP-9 null mice obviously support this hypothesis at least for the involvement of MMP-9.

As shown in the present study, the development of edema was significantly observed after ischemic stress. Since many reports have also demonstrated the proteolytic degradation by MMP of critical blood-brain barrier contributes the development of post-ischemic edema (Asahi et al., 2001; Lee et al., 2004; Svedin et al., 2007), it is possible that NCAM is involved not only in the MMP-mediated development of ischemic neuronal damage but also in the MMP-mediated development of post-ischemic edema.

Although we could not distinguish which MMP (MMP-2 or MMP-9) is more important in ischemic stress-induced NCAM degradation in this study, our results indicate that their specificity against NCAM and the characteristic differences between MMP-2 and MMP-9 in the NCAM degradation may be small. Clinical report showing that proteolytic product of NCAM by MMP (65–70 kDa bands) increases under neuropathological conditions (Tanaka et al., 2007) is in agreement with our findings in the present study. Importantly, this is the first study demonstrating the MMP-mediated proteolysis of NCAM in a cerebral ischemic stress model animal. As demonstrated, the full length of NCAM (180 kDa) was significantly decreased on day 1 after MCAO and it recovered to the normal levels on day 3, while the protein levels of NCAM cleavage product (65 kDa) kept increasing until day 3. These results suggest that some physiological compensatory reaction against the down-regulation of NCAM (180 kDa) may occur after ischemic stress, while its cleavage reaction by MMP-2 and MMP-9 into NCAM cleavage product (65 kDa) continued. Furthermore, the transient decrease of full length NCAM (180 kDa) in the early phase of ischemic stress may be one of the important triggers in the development of neuronal damage. Note that MMP-9 inhibitor I is a potent and selective inhibitor of MMP-9, but also inhibits and MMP-13 and MMP-1 at higher concentrations, according to manufacture's instruction. Likewise, MMP-2

inhibitor III is a potent and selective inhibitor of MMP-2, but also inhibits and MMP-9 and MMP-3 at higher concentrations, suggesting the possible involvement of MMPs other than MMP-2 and MMP-9, while it remains to be determined.

The increase of fragment of NCAM (65–70 kDa) and the other fragment of NCAM (105–115 kDa) has been reported in patients with schizophrenia or Alzheimer's disease (Vawter, 2000; Todaro et al., 2004; Tanaka et al., 2007). Taken together, proteolysis of NCAM by MMP-dependent shedding (Hubschmann et al., 2005; Hinkle et al., 2006) may occur in neurodegenerative disorders. Although we did not determine the alterations of NCAM fragment (105–115 kDa) under ischemic stress, the present findings indicate that the MMP-mediated NCAM proteolysis may be implicated in the exacerbation of ischemic neuronal damage. Furthermore, it is possible that the accumulation of NCAM cleavage product is related to a deteriorative or degenerative process in ischemic neuronal damage as described in the case of schizophrenia (Vawter, 2000), however it remains to be determined.

In conclusion, we found that MMP-mediated decrease of full length NCAM (180 kDa) is a new mechanism for the development of ischemic neuronal damage. These findings may help the development of new drugs or therapeutic strategies against stroke in the future.

JPET #178079

Authorship Contributions

Participated in research design: Shichi, Fujita-Hamabe and Tokuyama

Conducted experiments: Shichi, Fujita-Hamabe, Harada and Tokuyama

Contributed new reagents or analytic tools: Mizoguchi, Yamada, Nabeshima and Tokuyama

Performed data analysis: Shichi, Fujita-Hamabe, Harada and Tokuyama

Wrote or contributed to the writing of the manuscript: Shichi, Fujita-Hamabe, Nabeshima and Tokuyama

References

- Amantea D, Russo R, Gliozzi M, Fratto V, Berliocchi L, Bagetta G, Bernardi G and Corasaniti MT (2007) Early upregulation of matrix metalloproteinases following reperfusion triggers neuroinflammatory mediators in brain ischemia in rat. *Int Rev Neurobiol* **82**:149-169.
- Asahi M, Wang X, Mori T, Sumii T, Jung JC, Moskowitz MA, Fini ME and Lo EH (2001) Effects of matrix metalloproteinase-9 gene knock-out on the proteolysis of blood-brain barrier and white matter components after cerebral ischemia. *J Neurosci* **21**: 7724-7732.
- Berezin V, Bock E and Poulsen FM (2000) The neural cell adhesion molecule. *Curr Opin Drug Discov Devel* **3**:605-609.
- Bisaz R, Conboy L and Sandi C (2009) Learning under stress: a role for the neural cell adhesion molecule NCAM. *Neurobiol Learn Mem* **91**:333-342.
- Bukalo O, Fentrop N, Lee AY, Salmen B, Law JW, Wotjak CT, Schweizer M, Dityatev A and Schachner M (2004) Conditional ablation of the neural cell adhesion molecule reduces precision of spatial learning, long-term potentiation, and depression in the CA1 subfield of mouse hippocampus. *J Neurosci* **24**:1565-1577.
- Chadi G, Maximino JR and de Oliveira GP (2009) The importance of molecular histology

JPET #178079

to study glial influence on neurodegenerative disorders. Focus on recent developed single cell laser microdissection. *J Mol Histol* **40**:241-250.

Conant K, Wang Y, Szklarczyk A, Dudak A, Mattson MP and Lim ST (2010) Matrix metalloproteinase-dependent shedding of intercellular adhesion molecule-5 occurs with long-term potentiation. *Neuroscience* **166**:508-521.

Cremer H, Chazal G, Carleton A, Goridis C, Vincent JD and Lledo PM (1998) Long-term but not short-term plasticity at mossy fiber synapses is impaired in neural cell adhesion molecule-deficient mice. *Proc Natl Acad Sci U S A* **95**:13242-13247.

Cremer H, Lange R, Christoph A, Plomann M, Vopper G, Roes J, Brown R, Baldwin S, Kraemer P, Scheff S and et al. (1994) Inactivation of the N-CAM gene in mice results in size reduction of the olfactory bulb and deficits in spatial learning. *Nature* **367**:455-459.

del Zoppo GJ, Milner R, Mabuchi T, Hung S, Wang X, Berg GI and Koziol JA (2007) Microglial activation and matrix protease generation during focal cerebral ischemia. *Stroke* **38**:646-651.

Ding-Zhou L, Marchand-Verrecchia C, Palmier B, Croci N, Chabrier PE, Plotkine M and Margail I (2003) Neuroprotective effects of (S)-N-[4-[4-[(3,4-Dihydro-6-hydroxy-2,5,7,8-tetramethyl-2H-1-benzopyran-2-

JPET #178079

yl)carbonyl]-1-piperazinyl]phenyl]-2-thiophenecarboximid-amide (BN 80933), an inhibitor of neuronal nitric-oxide synthase and an antioxidant, in model of transient focal cerebral ischemia in mice. *J Pharmacol Exp Ther* **306**:588-594.

Doherty P, Williams G and Williams EJ (2000) CAMs and axonal growth: a critical evaluation of the role of calcium and the MAPK cascade. *Mol Cell Neurosci* **16**:283-295.

Franklin KBJ and Paxinos G (2008) *The mouse brain in stereotaxic coordinates*, 3rd ed. Academic Press, New York.

Gu Z, Cui J, Brown S, Fridman R, Mobashery S, Strongin AY and Lipton SA (2005) A highly specific inhibitor of matrix metalloproteinase-9 rescues laminin from proteolysis and neurons from apoptosis in transient focal cerebral ischemia. *J Neurosci* **25**:6401-6408.

Haley TJ and McCormick WG (1957) Pharmacological effects produced by intracerebral injection of drugs in the conscious mouse. *Br J Pharmacol Chemother* **12**:12-15.

Hankey GJ and Warlow CP (1999) Treatment and secondary prevention of stroke: evidence, costs, and effects on individuals and populations. *Lancet* **354**:1457-1463.

Harada S, Fujita-Hamabe W and Tokuyama S (2010) The importance of regulation of blood glucose levels through activation of peripheral 5'-AMP-activated protein kinase on ischemic neuronal damage. *Brain Res* **1351**: 254-263.

Harada S, Hamabe W, Kamiya K, Satake T, Yamamoto J and Tokuyama S (2009) Preventive effect of *Morinda citrifolia* fruit juice on neuronal damage induced by focal ischemia. *Biol Pharm Bull* **32**:405-409.

Hasegawa Y, Morioka M, Hasegawa S, Matsumoto J, Kawano T, Kai Y, Yano S, Fukunaga K and Kuratsu J (2006) Therapeutic time window and dose dependence of neuroprotective effects of sodium orthovanadate following transient middle cerebral artery occlusion in rats. *J Pharmacol Exp Ther* **317**:875-881.

Heo JH, Lucero J, Abumiya T, Koziol JA, Copeland BR and del Zoppo GJ (1999) Matrix metalloproteinases increase very early during experimental focal cerebral ischemia. *J Cereb Blood Flow Metab* **19**:624-633.

Hinkle CL, Diestel S, Lieberman J and Maness PF (2006) Metalloprotease-induced ectodomain shedding of neural cell adhesion molecule (NCAM). *J Neurobiol* **66**:1378-1395.

Hubschmann MV, Skladchikova G, Bock E and Berezin V (2005) Neural cell adhesion molecule function is regulated by metalloproteinase-mediated ectodomain release.

J Neurosci Res **80**:826-837.

Kawasaki Y, Xu ZZ, Wang X, Park JY, Zhuang ZY, Tan PH, Gao YJ, Roy K, Corfas G, Lo EH and Ji RR (2008) Distinct roles of matrix metalloproteases in the early- and late-phase development of neuropathic pain. *Nat Med* **14**:331-336.

Kiryushko D, Berezin V and Bock E (2004) Regulators of neurite outgrowth: role of cell adhesion molecules. *Ann N Y Acad Sci* **1014**:140-154.

Koistinaho M, Malm TM, Kettunen MI, Goldsteins G, Starckx S, Kauppinen RA, Opendakker G and Koistinaho J (2005) Minocycline protects against permanent cerebral ischemia in wild type but not in matrix metalloprotease-9-deficient mice.

J Cereb Blood Flow Metab **25**: 460-467.

Lee SR, Tsuji K, Lee SR and Lo EH (2004) Role of matrix metalloproteinases in delayed neuronal damage after transient global cerebral ischemia *J Neurosci* **24**: 671-678.

Liu X, Zhang W, Alkayed NJ, Froehner SC, Adams ME, Amiry-Moghaddam M, Ottersen OP, Hurn PD and Bhardwaj A (2008) Lack of sex-linked differences in cerebral edema and aquaporin-4 expression after experimental stroke. *J Cereb Blood Flow Metab* **28**:1898-1906.

- Macas J, Nern C, Plate KH and Momma S (2006) Increased generation of neuronal progenitors after ischemic injury in the aged adult human forebrain. *J Neurosci* **26**:13114-13119.
- Maness PF and Schachner M (2007) Neural recognition molecules of the immunoglobulin superfamily: signaling transducers of axon guidance and neuronal migration. *Nat Neurosci* **10**:19-26.
- Mizoguchi H, Yamada K, Mouri A, Niwa M, Mizuno T, Noda Y, Nitta A, Itohara S, Banno Y and Nabeshima T (2007) Role of matrix metalloproteinase and tissue inhibitor of MMP in methamphetamine-induced behavioral sensitization and reward: implications for dopamine receptor down-regulation and dopamine release. *J Neurochem* **102**:1548-1560.
- Mizoguchi H, Yamada K and Nabeshima T (2008) Neuropsychotoxicity of abused drugs: involvement of matrix metalloproteinase-2 and -9 and tissue inhibitor of matrix metalloproteinase-2 in methamphetamine-induced behavioral sensitization and reward in rodents. *J Pharmacol Sci* **106**:9-14.
- Poltorak M, Frye MA, Wright R, Hemperly JJ, George MS, Pazzaglia PJ, Jerrels SA, Post RM and Freed WJ (1996) Increased neural cell adhesion molecule in the CSF of patients with mood disorder. *J Neurochem* **66**:1532-1538.

JPET #178079

- Povlsen GK, Ditlevsen DK, Berezin V and Bock E (2003) Intracellular signaling by the neural cell adhesion molecule. *Neurochem Res* **28**:127-141.
- Ronn LC, Hartz BP and Bock E (1998) The neural cell adhesion molecule (NCAM) in development and plasticity of the nervous system. *Exp Gerontol* **33**:853-864.
- Sarabi AS, Shen H, Wang Y, Hoffer BJ and Backman CM (2008) Gene expression patterns in mouse cortical penumbra after focal ischemic brain injury and reperfusion. *J Neurosci Res* **86**:2912-2924.
- Shinohara Y, Nagayama M and Origasa H (2009) Postpublication external review of the Japanese guidelines for the management of stroke 2004. *Stroke* **40**:1439-1443.
- Svedin P, Hagberg H, Sävmán K, Zhu C and Mallard C (2007) Matrix metalloproteinase-9 gene knock-out protects the immature brain after cerebral hypoxia-ischemia. *J Neurosci* **27**: 1511-1518.
- Szklarczyk A, Lapinska J, Rylski M, McKay RD and Kaczmarek L (2002) Matrix metalloproteinase-9 undergoes expression and activation during dendritic remodeling in adult hippocampus. *J Neurosci* **22**:920-930.
- Tacke R and Goridis C (1991) Alternative splicing in the neural cell adhesion molecule pre-mRNA: regulation of exon 18 skipping depends on the 5'-splice site. *Genes Dev* **5**:1416-1429.

JPET #178079

Tanaka Y, Yoshida S, Shimada Y, Ueda H and Asai K (2007) Alteration in serum neural cell adhesion molecule in patients of schizophrenia. *Hum Psychopharmacol* **22**:97-102.

Todaro L, Puricelli L, Gioseffi H, Guadalupe Pallotta M, Lastiri J, Bal de Kier Joffe E, Varela M and Sacerdote de Lustig E (2004) Neural cell adhesion molecule in human serum. Increased levels in dementia of the Alzheimer type. *Neurobiol Dis* **15**:387-393.

Vawter MP (2000) Dysregulation of the neural cell adhesion molecule and neuropsychiatric disorders. *Eur J Pharmacol* **405**:385-395.

Yagi K, Kitazato KT, Uno M, Tada Y, Kinouchi T, Shimada K and Nagahiro S (2009) Edaravone, a free radical scavenger, inhibits MMP-9-related brain hemorrhage in rats treated with tissue plasminogen activator. *Stroke* **40**:626-631.

Yang G, Kitagawa K, Matsushita K, Mabuchi T, Yagita Y, Yanagihara T and Matsumoto M (1997) C57BL/6 strain is most susceptible to cerebral ischemia following bilateral common carotid occlusion among seven mouse strains: selective neuronal death in the murine transient forebrain ischemia. *Brain Res* **752**:209-218.

JPET #178079

Yepes M, Sandkvist M, Wong MK, Coleman TA, Smith E, Cohan SL and Lawrence DA

(2000) Neuroserpin reduces cerebral infarct volume and protects neurons from ischemia-induced apoptosis. *Blood* **96**:569-576.

Yong VW, Power C, Forsyth P and Edwards DR (2001) Metalloproteinases in biology

and pathology of the nervous system. *Nat Rev Neurosci* **2**:502-511.

Zhao BQ, Ikeda Y, Ihara H, Urano T, Fan W, Mikawa S, Suzuki Y, Kondo K, Sato K,

Nagai N and Umemura K (2004) Essential role of endogenous tissue plasminogen

activator through matrix metalloproteinase 9 induction and expression on

heparin-produced cerebral hemorrhage after cerebral ischemia in mice. *Blood*

103:2610-2616.

JPET #178079

Footnotes

This work was supported by the grants-in-aid and special coordination funds from

'Academic Frontier' Project, Cooperative Research Center of Life Sciences.

Figure legends

Fig. 1 Development of neuronal damage and protein levels of MMP-2 and MMP-9 in the cerebral cortex after cerebral ischemic stress. A, representative photographs of infarct volume. Three coronal sections at 0, +2, +4 mm from the bregma were stained with 2, 3, 5-triphenyltetrazolium (TTC) on indicated periods. B, quantitative analysis of the infarct volume (sham, n = 9; day 1, n = 9; day 3, n = 8). C, brain water content (sham, n = 10; day 1, n = 17; day 3, n = 18). * $p < 0.05$, one-way ANOVA and Scheffe's test. D, neurological examination was performed using the NDS. The boxes contain the values between the 25th and 75th percentile, the line across the boxes represent the medians, the whiskers extend to the highest and lowest values (day 1 sham, n = 9; day 1 MCAO, n = 9; day 3 sham, n = 9; day 3 MCAO, n = 8). ** $p < 0.01$, ## $p < 0.01$, Steel-Dwass test. E, MMP-2 protein levels (72 kDa) (day 1 sham, n = 11; day 1 MCAO, n = 16; day 3 sham, n = 14; day 3 MCAO, n = 20). F, MMP-9 protein levels (108 kDa) (day 1 sham, n = 11; day 1 MCAO, n = 16; day 3 sham, n = 14; day 3 MCAO, n = 20). The protein levels of MMP-2 and MMP-9 were analyzed by western blotting. The relative MMP-2/-9 levels were measured by determining a ratio between MMP-2/-9 and the endogenous internal standard protein GAPDH. Each column indicates the mean \pm S.E.M. ** $p < 0.01$, ## $p <$

JPET #178079

0.01, one-way ANOVA and Scheffe's test. G, representative photographs and semi-quantified data of MMP activities analyzed by gelatin zymography on day 3 after MCAO. Each column indicates the mean \pm S.E.M. (sham, n = 3; MCAO vehicle, n = 3; MCAO GM6001, n = 3) * p < 0.05, ** p < 0.01, # p < 0.05, ## p < 0.01, one-way ANOVA and Scheffe's test.

Fig. 2 Effect of NCAM siRNA on ischemic neuronal damage. A, effect of siRNA of NCAM on the protein levels of NCAM in naïve mice analyzed by western blotting. The relative NCAM levels were measured by determining a ratio between NCAM and the endogeneous internal standard protein GAPDH (control, n = 6; NCAM siRNA, n = 6). Each column indicates the mean \pm S.E.M. * p < 0.05, unpaired Student's t -test. B, representative photographs of infarct volume on day 1 after cerebral ischemic stress. C, quantitative analysis of the infarct volume (control, n = 9; NCAM siRNA, n = 10). * p < 0.05, unpaired Student's t -test. D, neurological examination was performed using the NDS. Results are expressed as the mean \pm S.E.M. (control, n = 9; NCAM siRNA, n = 10). ** p < 0.01, Steel-Dwass test.

Fig. 3 Protein levels of NCAM (180 kDa) and NCAM cleavage product (65 kDa) after

JPET #178079

cerebral ischemic stress. A, NCAM protein levels (180 kDa) (day 1 sham, n = 14; day 1 MCAO, n = 14; day 3 sham, n = 20; day 3 MCAO, n = 20). B, NCAM cleavage product levels (65 kDa) (day 1 sham, n = 5; day 1 MCAO, n = 10; day 3 sham, n = 20; day 3 MCAO, n = 22). The protein levels of NCAM were analyzed by western blotting. Each column indicates the mean \pm S.E.M. $**p < 0.01$, $## p < 0.01$, one-way ANOVA and Scheffe's test.

Fig. 4 Effect of a non-selective MMP inhibitor, GM6001, on ischemic neuronal damage, NCAM protein levels and NCAM cleavage product levels. A, representative photographs of infarct volume. B, quantitative analysis of the infarct volume (vehicle, n = 6; GM6001, n = 12). $##p < 0.01$, unpaired Student's *t*-test. C, neurological examination was performed using the NDS. Results are expressed as the mean \pm S.E.M. (sham, n = 6; vehicle, n = 6; GM6001, n = 12). $**p < 0.01$, $##p < 0.01$, Steel-Dwass test. D, NCAM protein levels (180 kDa), (sham, n = 9; vehicle, n = 28; GM6001, n = 28). E, NCAM cleavage product levels (65 kDa) (day 1 sham, n = 9; day 1 vehicle, n = 28; day 1 GM6001, n = 28; day 3 sham, n = 20; day 3 vehicle, n = 28; day 3 GM6001, n = 28). The protein levels of NCAM were analyzed by western blotting. Each column indicates the mean \pm S.E.M. $*p < 0.05$, $**p < 0.01$, $#p < 0.05$, $##p < 0.01$, one-way ANOVA and Scheffe's test.

Fig. 5 Effect of MMP-2 specific inhibitor III (MMP-2 III) on ischemic neuronal damage, NCAM protein levels and NCAM cleavage product levels. A, representative photographs of infarct volume on day 3. B, quantitative analysis of the infarct volume (vehicle, n = 10; MMP-2 III, n = 6). $##p < 0.01$, unpaired Student's *t*-test. C, neurological examination was performed using the NDS. Results are expressed as mean \pm S.E.M. (sham, n = 6; vehicle, n = 10; MMP-2 III, n = 6). $**p < 0.01$, $##p < 0.01$, Steel-Dwass test. D, NCAM protein levels (180 kDa) (sham, n = 10; vehicle, n = 10; MMP-2 III, n = 4). E, NCAM cleavage product levels (65 kDa) (day 1 sham, n = 10; day 1 vehicle, n = 10; day 1 MMP-2 III, n = 14; day 3 sham, n = 10; day 3 vehicle, n = 10; day 3 MMP-2 III, n = 14). The protein levels of NCAM were analyzed by western blotting. Each column indicates the mean \pm S.E.M. $*p < 0.05$, $**p < 0.01$, $##p < 0.01$, one-way ANOVA and Scheffe's test.

Fig. 6 Effect of MMP-9 specific inhibitor I (MMP-9 I) on ischemic neuronal damage, NCAM protein levels and NCAM cleavage product levels. A, representative photographs of infarct volume on day 3 after cerebral ischemic stress. B, quantitative analysis of the infarct volume (vehicle, n = 4; MMP-9 I, n = 13). Results are expressed as the mean \pm S.E.M. $##p < 0.01$, Student's *t*-test. C, neurological examination was performed using the

JPET #178079

NDS (sham, n = 4; vehicle, n = 4; MMP-9 I, n = 13). $**p < 0.01$, $##p < 0.01$, Steel-Dwass test. D, NCAM protein levels (180 kDa) (sham, n = 10; vehicle, n = 11; MMP-9 I, n = 14). E, NCAM cleavage product levels (65 kDa) (day 1 sham, n = 6; day 1 vehicle, n = 10; day 1 MMP-9 I, n = 10; day 3 sham, n = 10; day 3 vehicle, n = 14; day 3 MMP-9 I, n = 14). The protein levels of NCAM were analyzed by western blotting. Each column indicates mean \pm S.E.M. $*p < 0.05$; $**p < 0.01$, $##p < 0.01$, one-way ANOVA and Scheffe's test.

Fig. 7 Ischemic neuronal damage and NCAM protein levels, NCAM cleavage product levels after cerebral ischemic stress in MMP-9 KO mice. A, representative photographs of infarct volume. B, quantitative analysis of the infarct volume (WT, n = 9; MMP-9 KO, n = 10). $*p < 0.05$, unpaired Student's *t*-test. C, neurological examination was performed using the NDS. (WT, n = 3; MMP-9 KO, n = 4). $**p < 0.01$, Wilcoxon-Mann-Whitney U test. D, NCAM protein levels (180 kDa) (sham WT, n = 10; WT, n = 10; MMP-9 KO, n = 14). E, NCAM cleavage product levels (65 kDa) (sham WT, n = 6; WT, n = 14; MMP-9 KO, n = 6). The protein levels of NCAM were analyzed by western blotting. Each column indicates mean \pm S.E.M. $*p < 0.05$, $##p < 0.01$, one-way ANOVA and Scheffe's test.

Figure 1

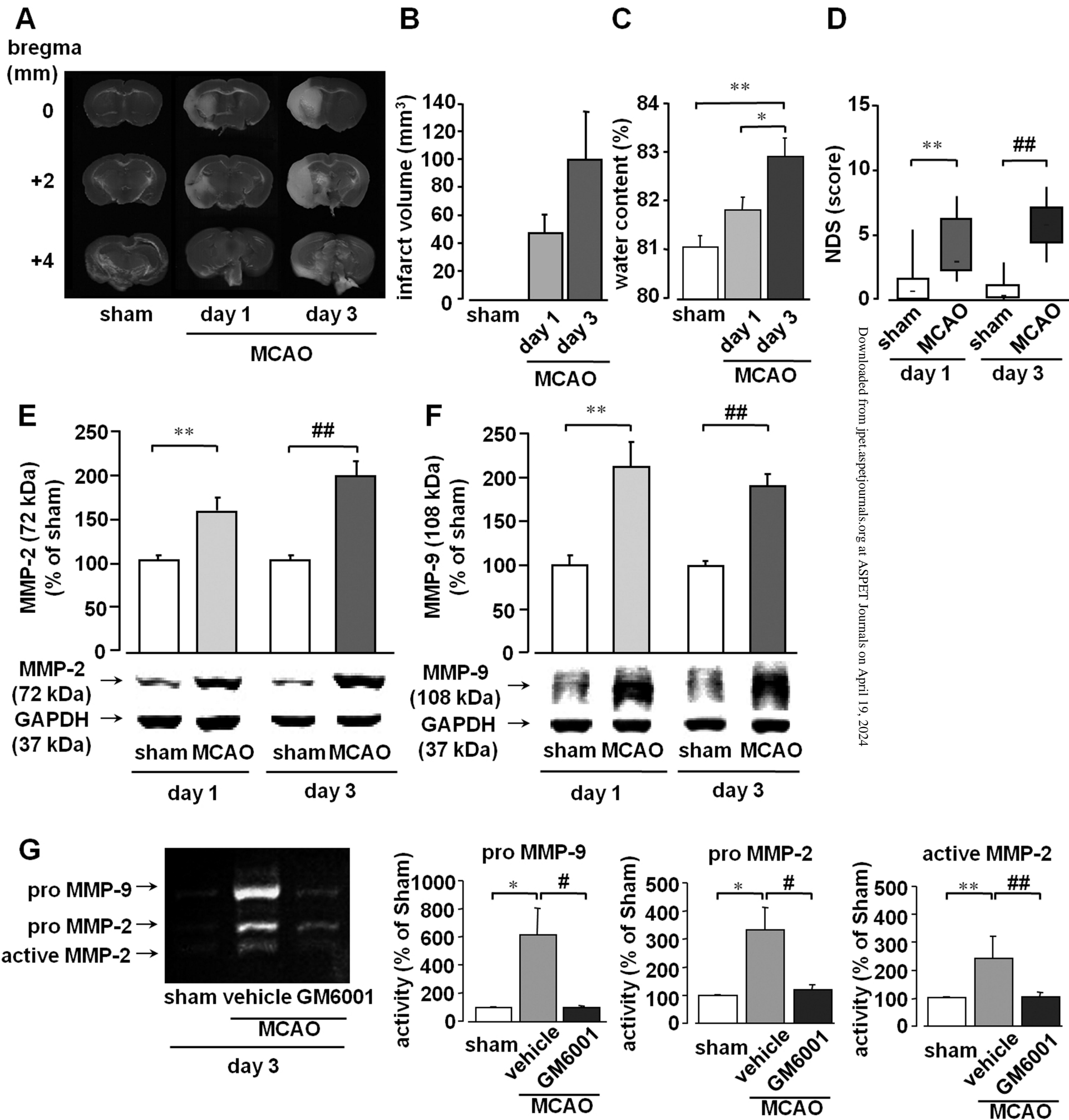


Figure 2

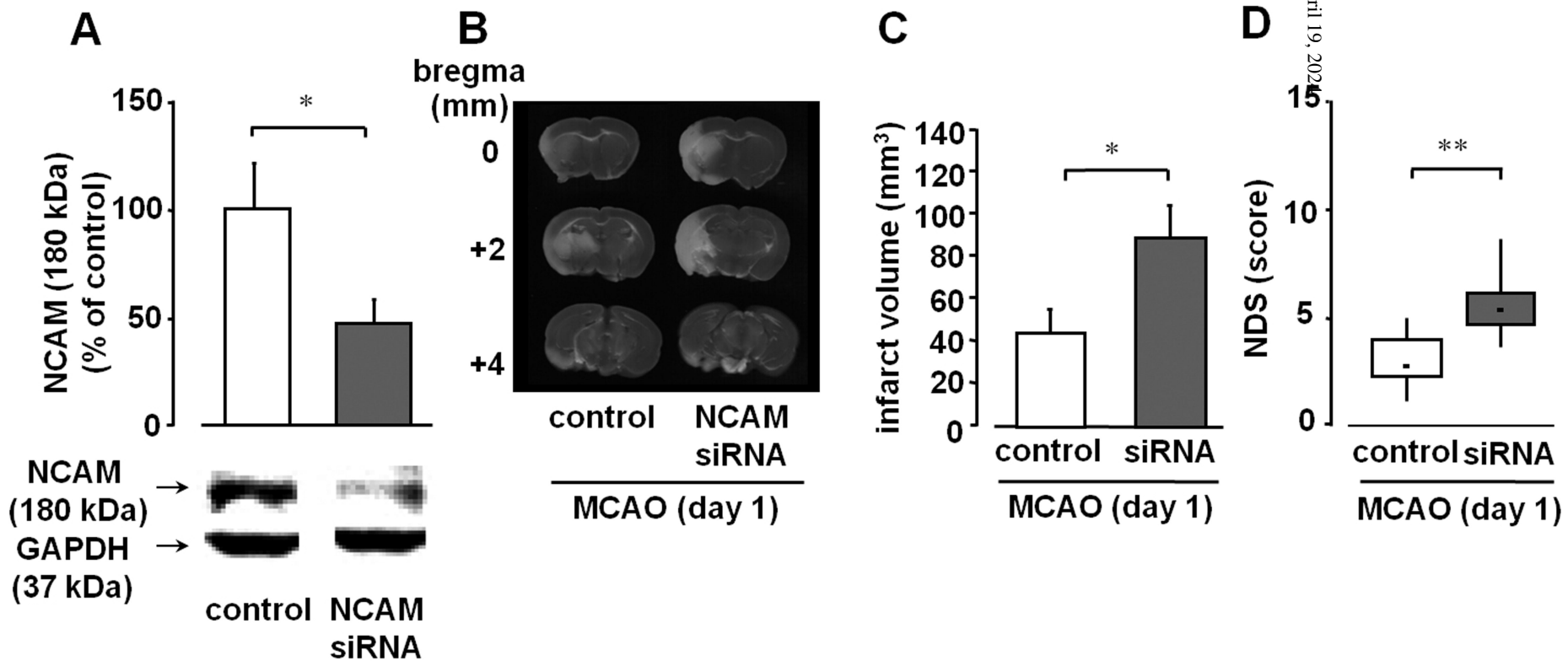


Figure 3

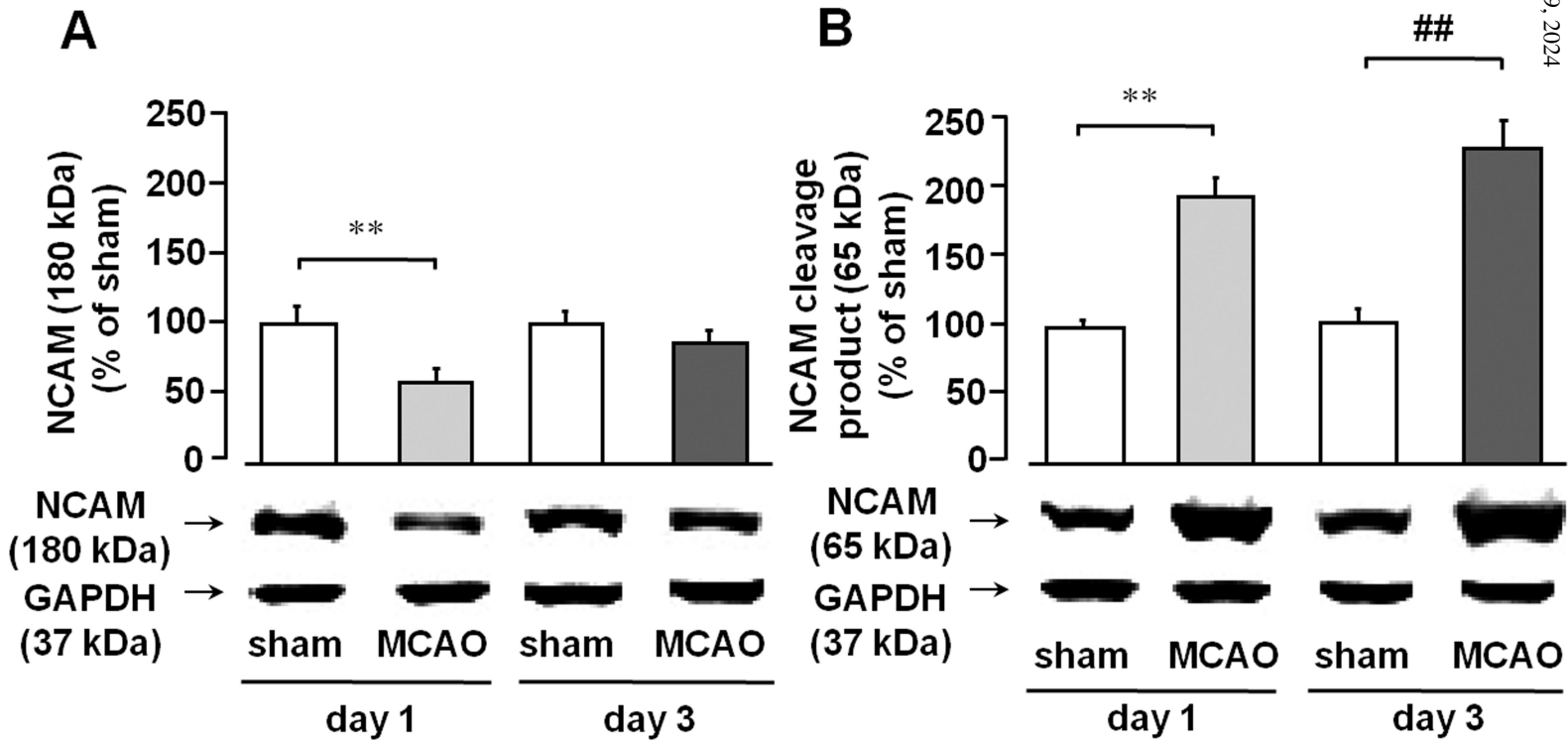


Figure 4

A

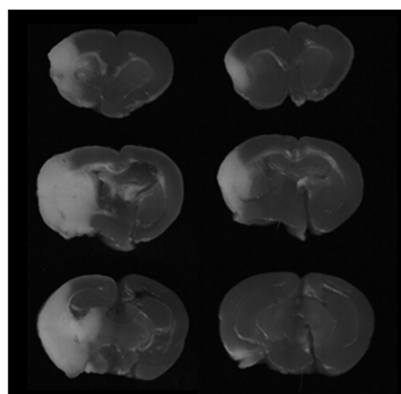
bregma

(mm)

0

+2

+4

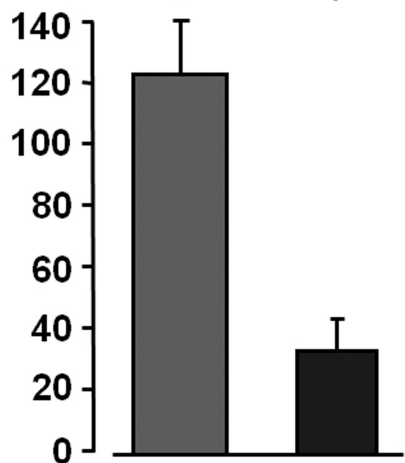


vehicle GM6001

MCAO (day 3)

B

infarct volume (mm³)

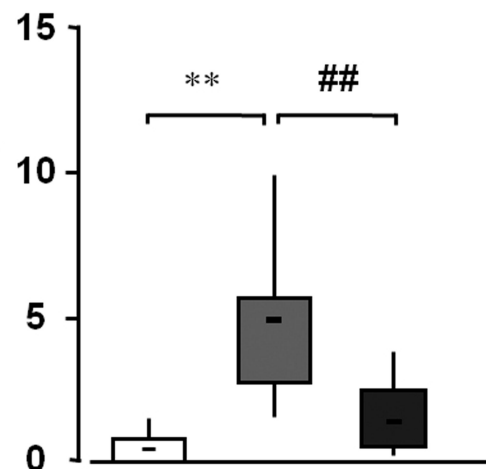


vehicle GM6001

MCAO (day 3)

C

NDS (score)

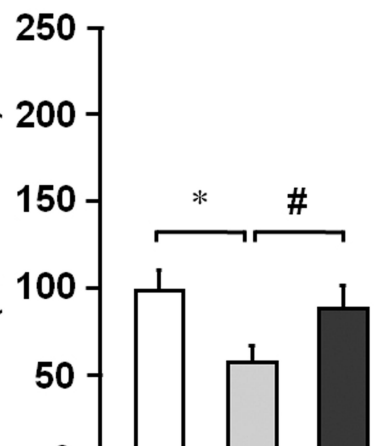


sham vehicle GM6001

MCAO (day 3)

D

NCAM (180 kDa)
(% of sham)

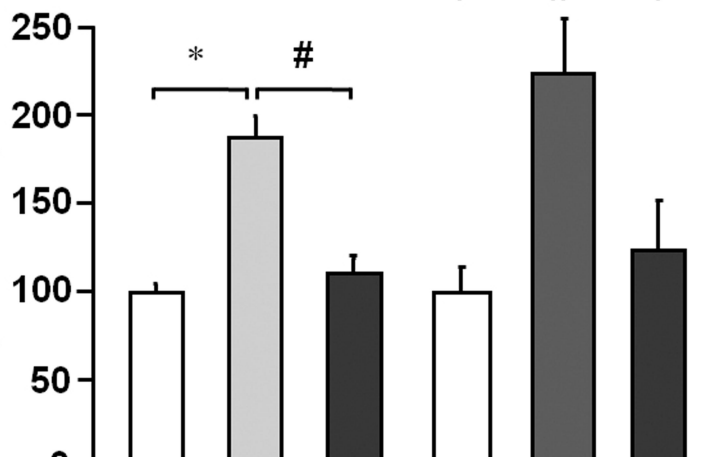


sham vehicle GM6001

MCAO
day 1

E

NCAM cleavage
product (65 kDa)
(% of sham)



sham vehicle GM6001 sham vehicle GM6001

MCAO
day 1

MCAO
day 3

Figure 5

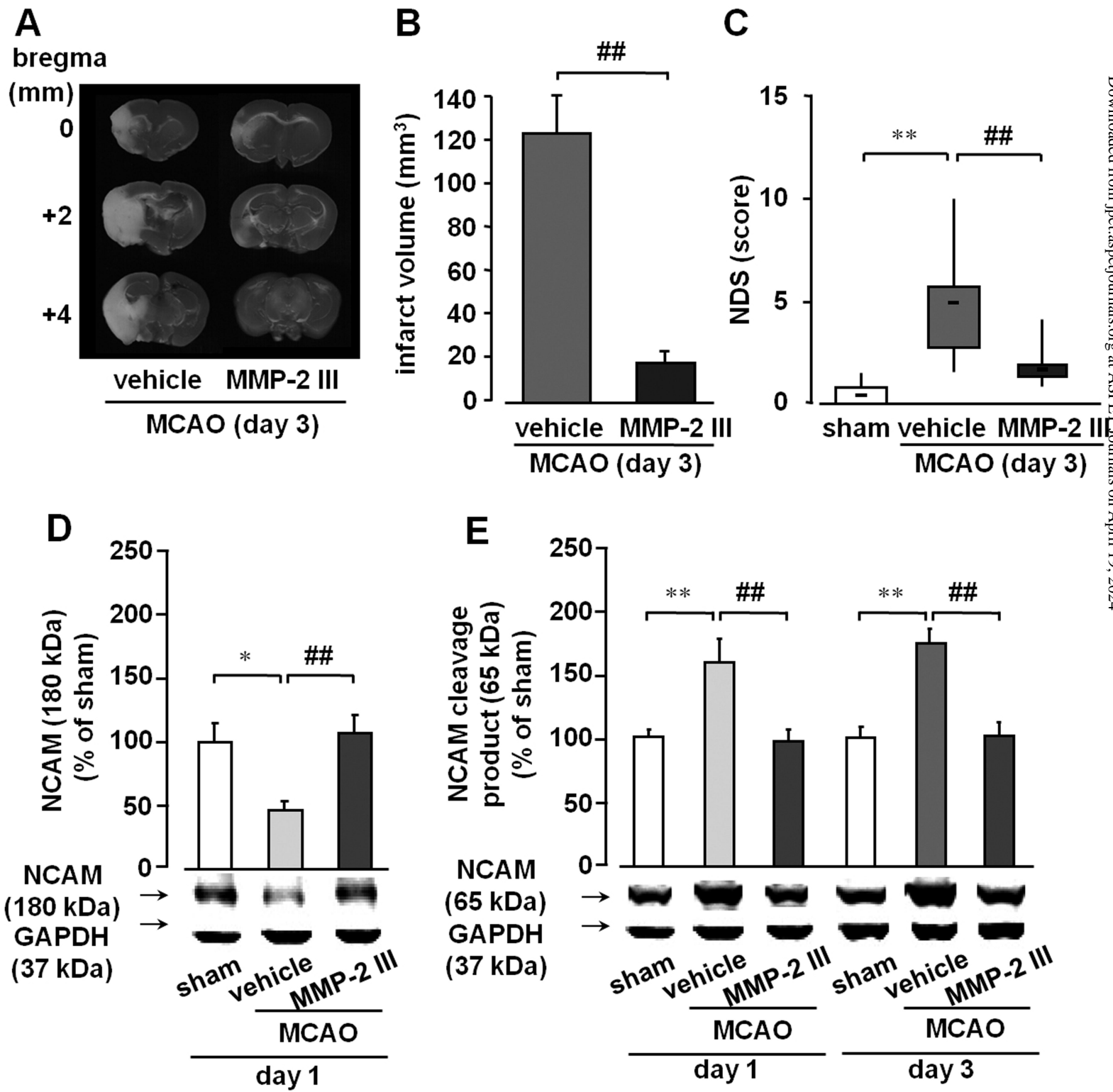


Figure 6

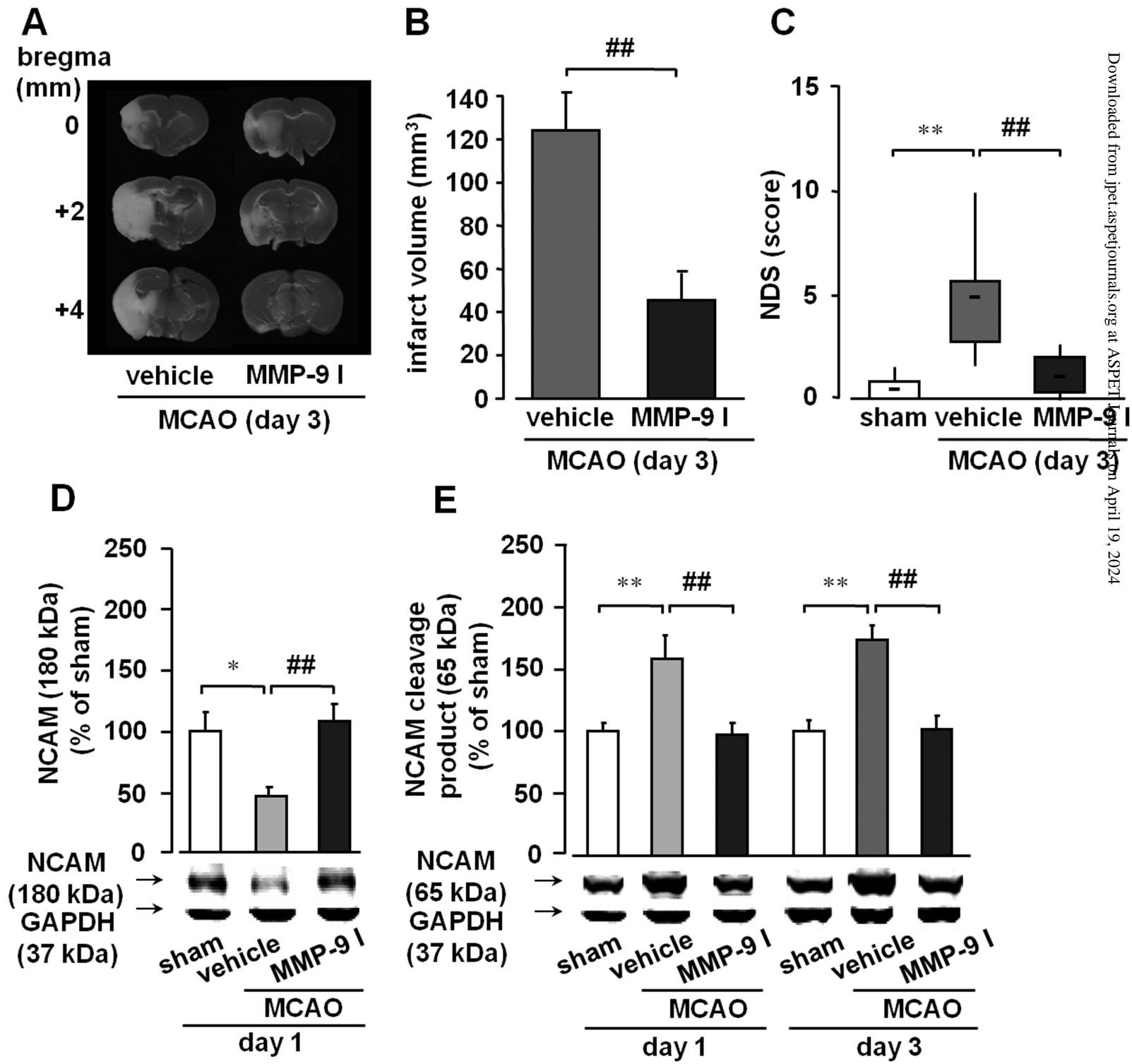


Figure 7

